Single-molecule conductance determinations on $HS(CH_2)_4O(CH_2)_4SH$ and $HS(CH_2)_2O(CH_2)_2O(CH_2)_2SH$, and comparison with alkanedithiols of the same length

2012 J. Phys.: Condens. Matter 24 164211

(http://iopscience.iop.org/0953-8984/24/16/164211)

J. Phys.: Condens. Matter **24** (2012) 164211 (9pp) doi:10.1088/0953-8984/24/16/164211

Single-molecule conductance determinations on $HS(CH_2)_4O(CH_2)_4SH$ and $HS(CH_2)_2O(CH_2)_2O(CH_2)_2SH$, and comparison with alkanedithiols of the same length*

Lisa E Scullion, Edmund Leary[1], Simon J Higgins and Richard J Nichols

Department of Chemistry, University of Liverpool, Crown Street, Liverpool L69 7ZD, UK

E-mail: shiggins@liv.ac.uk

Received 8 April 2011, in final form 17 June 2011
Published 30 March 2012
Online at stacks.iop.org/JPhysCM/24/164211

Abstract

The acetyl-protected, thiol-terminated ethers $AcS(CH_2)_4O(CH_2)_4SAc$ and $AcS(CH_2)_2O(CH_2)_2O(CH_2)_2SAc$ have been synthesised, and a range of related scanning tunnelling microscopy (STM)-based methods have been employed to fabricate and electrically characterise gold | single molecule | gold junctions involving these molecules. The single-molecule conductance values obtained are consistently found to be substantially higher (by a factor of 2–3) than the conductances of analogous alkanedithiols of similar length ($HS(CH_2)_9SH$ and $HS(CH_2)_8SH$, respectively). A rationalisation of these findings is suggested, namely that the lone pair electrons on the oxygen atoms are substantially closer in energy to the Fermi energy of the gold leads than are the occupied and unoccupied states of methylene chains, so that the ether oxygens behave in a manner analogous to 'wells' in a double-tunnelling-barrier system. In agreement with this suggestion, the current–voltage behaviour of the monoether can be fitted using the Simmons approach, and the barrier height is found to be significantly lower than for alkanedithiols of approximately the same length.

S Online supplementary data available from stacks.iop.org/JPhysCM/24/164211/mmedia

(Some figures in this article are in colour only in the electronic version)

1. Introduction

The last decade has witnessed the successful development of techniques for measuring the electrical properties of metal | molecule | metal junctions. These techniques include mechanically controlled break junctions, in which a nanoscale gap between two electrodes is created by using a bending force to break an ultrathin wire, following which molecules bearing suitable contact groups can successfully bridge the gap [1–6]. Molecular junctions can also be formed by scanning probe microscopy techniques, based on either scanning tunnelling microscopy [7–11] or conducting atomic force microscopy [12, 13]. For example, in an early study, Cui *et al* embedded a small fraction of alkanedithiol molecules, $HS(CH_2)_nSH$, into a close-packed, self-assembled layer of alkanemonothiol, $HS(CH_2)_nCH_3$, on Au surfaces, and then used the 'free' thiol groups to trap gold nanoparticles. A conducting AFM was then used to first locate, and then make electrical contact with, the resulting Au | molecule | Au junction [12]. Subsequently we [10], and others [8], reported

* To Stuart Lindsay, in appreciation of his contributions to the field and of our lively discussions at various conferences.

[1] Present address: IMDEA, UAM, Facultad de Ciencias, Modulo C13, planta 3, Avenida Tomas y Valiente, 7, Ciudad Universitaria de Cantoblanco, E-28049 Madrid, Spain.

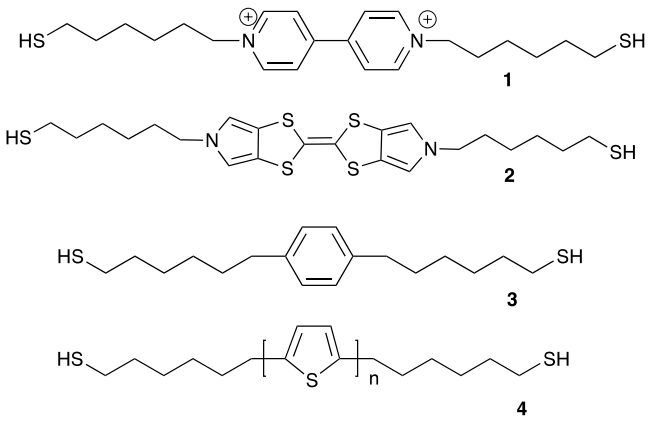

Figure 1. Structures of molecules **1**–**4**.

the formation of metal | molecule | metal junctions made by bringing a gold STM tip either into close proximity to, or into contact with, a gold substrate in the presence of dithiol molecules, followed by vertical withdrawal of the tip with simultaneous measurement of tunnelling current as the dithiol is extended into the resulting gap.

These developments have produced a plethora of studies to establish structure–property relations in single-molecule electrical properties, over the course of which it has become clear that the electrical properties of the junctions are not solely dependent upon the nature of the molecular backbone, but on many other factors, for example the electrodes, the detailed nature of the hybridisation at the molecule–electrode interfaces [14–18], the temperature [19, 20] and, in certain cases, the local environment (vacuum or air, solvent, etc) [21, 22].

We have been particularly interested in systems in which the electrical properties of metal | molecule | metal junctions can be controlled by an external stimulus, for example change in conformation using photochemical switching [23], pH control [24] and, especially, change in oxidation state using electrochemical switching [10, 25–27]. A key finding from the latter work, relevant to the present study, is that the conductance of junctions involving both molecules **1** and **2** (figure 1) are similar (0.5 and 0.7 nS, respectively); on reduction (**1**; to $V^{\bullet+}$) [10, 25, 26] or oxidation (**2**; to p-$TTF^{\bullet+}$) [27] the conductance increases as the relevant frontier molecular orbital (localised on the respective π systems) comes nearer to resonance with the Fermi energy of the metal contacts [26].

The conductances of **1** and **2**, even in their 'off' (non-near-resonant) states, are surprisingly high considering the length of the molecules. Since the frontier molecular orbitals of alkanedithiols are far from the Fermi energy of the metal contacts, the mechanism of conductance is tunnelling, and their conductance accordingly falls exponentially as a function of molecular length. For comparison with **1** and **2**, it should be noted that the conductance of $HS(CH_2)_6SH$ is 2.5 nS and that of $HS(CH_2)_{12}SH$ (i.e. the two alkylthiol linkers of **1** and **2** placed back-to-back) is 0.038 nS [28]. Therefore, although **1** and **2** are even longer than $HS(CH_2)_{12}SH$, their conductance, measured in ambient, is approximately an

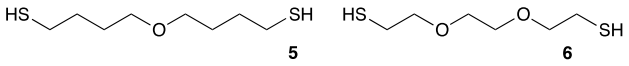

Figure 2. Monoether molecule **5** and diether molecule **6**.

order of magnitude greater. We have rationalised this by drawing an analogy with inorganic 'double-tunnelling-barrier' systems [29]. These have been introduced into field effect transistors [30], diodes [31–33] and bipolar transistors [34]. In these inorganic devices, metal–organic vapour phase epitaxy is used to assemble a 'well' or barrier indentation (a low-bandgap III–V semiconductor), sandwiched between the tunnelling barriers (higher-bandgap III–V semiconductors). In **1** and **2**, clearly the alkanethiol linkers will have a wider 'bandgap' (i.e. HOMO–LUMO separation) than the central conjugated π system.

Later, we showed that a simple arene ring (e.g. 1,4-phenyl or 2,5-thienyl), although not conventionally redox-active, is similarly capable of acting as a 'well'; junctions involving molecules **3** and **4** (figure 1; $n = 1$), for instance, have conductances similar to those involving **1** and **2** in their 'off' states [22, 35]. For molecules of the type **3**, we also showed that the conductance was significantly higher if electron-donating substituents were present and lower for electron-withdrawing substituents [35].

These results prompted us to wonder what are the minimum structural requirements for an entity to act as a 'well' in these molecules. Accordingly, we have now examined the conductances of junctions with monoether **5** and diether **6** (figure 2) in which ether oxygens, bearing non-bonded lone pairs of electrons, take the place of the arene unit.

Using close-packed, self-assembled monolayers of $HS(CH_2)_n–O–(CH_2)_mOH$ ($n = 6$; $m = 7$; $n = 7$, $m = 6$) and $HO(CH_2)_{14}SH$, Cheng *et al* found that the replacement of one $–CH_2–$ by an ether –O– significantly lowered the electrochemically determined electron transfer rate constants for solution species ($[Fe(CN)_6]^{3-}$ and $[Os(2,2'\text{-bipyridine})_3]^{3+}$) [36], while Napper *et al* came to the same conclusion in similar studies involving ferrocene-terminated monolayers, $FcC(O)O(CH_2)_5–O–(CH_2)_6SH$ or $FcC(O)O(CH_2)_{12}SH$ [Fc = $(\eta^5–C_5H_5)Fe(\eta^5–C_5H_4–)$], diluted into host matrices of $CH_3(CH_2)_5–O–(CH_2)_6SH$ or $CH_3(CH_2)_{11}SH$ [37]. In contrast, we now find, using careful examination of the conductance of junctions involving monoether **5** and diether **6** by several related but different techniques, that single-molecule junctions involving these ethers are significantly more conductive than are those involving alkanedithiols of comparable length (for **5**, $HS(CH_2)_9SH$ and for **6**, $HS(CH_2)_8SH$). We report these studies here.

2. Experimental section

2.1. Synthesis

Monoether **5** was prepared by the route shown in scheme 1 [38]. Diether **6** was prepared by treatment of commercial tri(ethylene glycol) di-*p*-toluenesulfonate with KSAc/acetone. The identity and purity of **5** and **6** were determined using

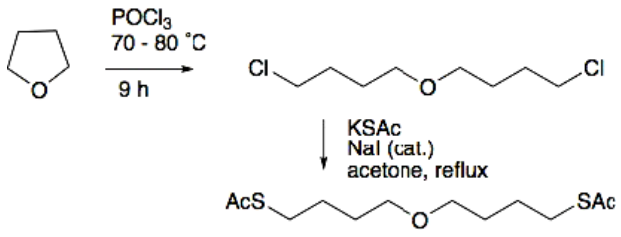

Scheme 1. Synthesis of the acetyl-protected **5**.

analytical and spectroscopic techniques. Full details are given in the supplementary information (available at stacks.iop.org/JPhysCM/24/164211/mmedia).

2.2. Single-molecule junction conductance determination: general remarks

Chromium primed gold on glass slides (Arrandee) were flame-annealed (butane/air) to produce Au(111) terraces. Following cooling, these substrates were immersed into a solution of the appropriate dithioacetate molecule (0.1 mM in CH_2Cl_2) for 1–2 min to produce the 'low-coverage' monolayer employed for the $I(s)$ and STM break junction experiments. The 'high-coverage' monolayers were prepared by increasing the exposure time to 24 h. The substrate was then washed with pure solvent, dried in an N_2 stream and mounted on the STM stage. The STM tips were made by cutting gold wire (0.25 mm diameter; Goodfellow, 99.99%); for some experiments where imaging was performed, the tips were prepared by electrochemical etching of the wire in a 50:50 v:v HCl:EtOH solution. For experiments conducted in water, the tips were coated with Apiezon wax, ensuring that only the tip apex was exposed.

For the diether **6**, XPS spectra were recorded on both low-coverage and high-coverage monolayers on identical substrates to those used in conductance determinations. Spectra were acquired using a Scienta ESCA 300 spectrometer (NCESS, Daresbury Laboratory, UK) at 90° take-off angle. The spectra were referenced to the main C–H 1s peak at 285.0 eV. A survey scan (0–1300 eV) was run, followed by high-resolution scans at characteristic peak positions for C, O and S.

2.3. I(s) experiments [10, 39]

The gold STM tip was brought within tunnelling distance of the substrate bearing a low-coverage monolayer, prepared as above, at an initial vertical distance controlled by the set-point current, I_0. The feedback loop was disconnected, a bias voltage applied and the tip was then withdrawn (total distance 6 nm; 0.1 s) while the current was measured as a function of vertical distance (hence $I(s)$; I = current, s = vertical distance). The feedback loop was then restored and the tip was moved back to the same initial I_0. For each molecule, we employed several I_0 values and different tip–substrate biases (section 3). For each set of parameters, the experiment was repeated many times (typically 500). Those current–distance curves showing clear plateaux (typically 100–200 for each set of conditions) were analysed statistically using a histogram plot of the current within a given range (determined by bin size) versus the frequency with which these occur. The break-off distance (the point at which the current plateau decays rapidly, as a consequence of the metal | molecule | metal junctions breaking on retraction) were similarly analysed statistically [18]. By adding a correction for the initial vertical height, the length of the junction prior to its breakdown can be determined. The procedure for making this correction has been previously described in detail [40]; in essence, it consists of analysing $I(s)$ curves in which only an exponential decay of current with distance is seen (i.e. in which no metal | molecule | metal junction is formed) and extrapolating the current–distance curve back to a current corresponding to the quantum conductance, G_0 ($G_0 = 2e^2/h = 77.4\ \mu$S). Further details are given in the supplementary information (available at stacks.iop.org/JPhysCM/24/164211/mmedia).

2.4. The STM 'break junction' method [8, 39]

Using an adaptation of the original STM technique devised by Xu *et al* for molecular junction formation [8], the STM tip was pushed into metallic contact with a low-coverage monolayer-coated Au(111) substrate ($z = -2$ nm) and was then retracted to $z = +6$ nm as for the $I(s)$ method while monitoring current. Current plateaux corresponding to the cleavage of metal | molecule | metal junctions, formed upon breaking the gold atomic contacts, were observed. The latter were analysed statistically as for the $I(s)$ method.

2.5. The compact monolayer I(s) method [41] ('Sek adaptation') [41]

The Au(111) substrate prepared as above was exposed to a 0.1 mM solution of monoether **5** or diether **6** for 24 h to allow the formation of a compact, upright-standing self-assembled monolayer. This was employed in $I(s)$ measurements in which an initial I_0 of 1 nA was chosen to place the tip just above the monolayer. The value of I_0 was then increased in 0.5 nA increments until $I(s)$ retraction curves began to show plateaux indicative of junction formation. For monoether **5** this occurred at $I_0 = 2$ nA, whereas for diether **6** I_0 was 5 nm. The experiment was then conducted as for the conventional $I(s)$ technique above, and the results were similarly analysed statistically.

3. Results and discussion

3.1. Single-molecule conductance determinations in ambient conditions: I(s) measurements

It has become clear in recent years that metal | molecule | metal junctions can exhibit different conductance values, depending upon the exact nature of the bonding between the contact atom(s) and the metal surfaces. We, and others, have identified the occurrence of three different conductance values for the same dithiol molecule [11, 17, 18, 42–44], and similar observations have since been reported for other contact groups,

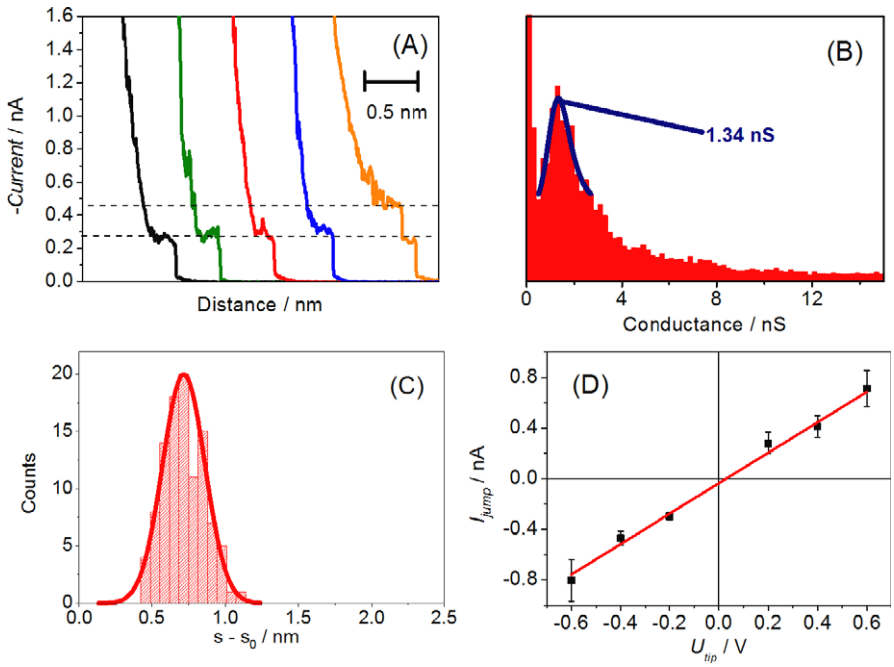

Figure 3. (A) Representative examples of I–s curves where a molecule bridges tip and substrate, illustrating I–s plateaux for $I(s)$ experiments using monoether **5** with $I_0 = 20$ nA and bias voltage $U_{tip} = 0.2$ V. (B) All-current-values histogram plot for the 100 $I(s)$ experiments in which a plateau such as the examples in (A) was obtained; the marked peak corresponds to the current value for single-molecule junctions involving **5** coordinated to low-coordination sites at both contact atoms. (C) Detachment histogram plot for this series of experiments; the average junction breakdown distance was 0.71 ± 0.12 nm and the correction for the initial vertical height was 0.71 nm, giving a mean detachment distance of 1.42 ± 0.12 nm; the S $\cdots$ S distance in **5** in its all-*trans* configuration, calculated using Spartan, is 1.31 nm. (D) Current–voltage plot from six $I(s)$ experiments of the type illustrated in (a)–(c) made at different values of U_{tip}.

such as pyridyl [45–47] and carboxylate [48]. In a detailed study of alkanedithiols using several different methods of forming junctions, we showed that there is a correlation between metal surface roughness and the frequency with which the higher conductance groups occur, suggesting that more highly coordinated contact atoms, more prevalent on rougher surfaces, give rise to higher conductance junctions [18]; this and earlier studies have formed the subject of a recent review [39]. In the present study, we have therefore focused on the lowest conductance group. By employing several techniques, including the STM break junction method that is known to favour junction formation involving the higher-coordinated contact atoms (resulting in the higher conductance groups) [18, 44], we have been able to cross-check the assignment of these lower conductance groups.

The conductances of junctions involving monoether **5** and diether **6** were first measured using the $I(s)$ technique (experimental; figures 3 and S1 (available at stacks.iop.org/JPhysCM/24/164211/mmedia), respectively) [10, 39]. If a molecule is trapped between the tip and substrate, the current at a given vertical height s is larger than that in the absence of a molecule, and at least one plateau is seen in the current–distance plot during tip retraction. Typical examples for **5** are shown in figure 3(A).

Owing to the fact that there is no control over the number of molecules in the junction, or the nature of the two metal | molecule contacts, the experiment must be repeated many times, and the results are analysed statistically using a histogram plot of the current versus the frequency with which this current occurs. Figure 3(B) illustrates this for one series of $I(s)$ experiments using monoether **5** (equivalent data for diether **6** is in the supplementary information, figure S1, available at stacks.iop.org/JPhysCM/24/164211/mmedia) [18, 39]. To check that the experiment is indeed addressing junctions involving individual molecules of **5** coordinated to low-coordination sites on the gold surfaces, a histogram of junction breakdown distances was also obtained (figure 3(C)); the mean junction breakdown distance (corrected for the initial vertical height of the tip, s_0) with this value of I_0 was 1.42 ± 0.12 nm, which compares favourably with an S $\cdots$ S distance for the all-*trans* conformation of **5** of 1.31 nm, calculated using the DFT implementation in Spartan 08.

A further advantage of the $I(s)$ technique is that one has control over the initial set-point current I_0, and hence over the initial tip height. We carried out experiments at I_0 values of 5, 20 and 60 nA. There was no difference, within experimental uncertainty, in the conductances of junctions involving **5** or **6** at these different I_0.

3.2. Junction formation using the 'push to contact' approach

Next, we measured the conductances of gold | molecule | gold junctions involving **5** and **6** by employing the STM 'push to contact' approach, first described by Xu *et al* [8]. Here, the STM tip is deliberately brought into contact with the gold surface in the presence of the molecule under test, and is then retracted as in the $I(s)$ method. It is presumed that metallic contact between tip and substrate breaks upon

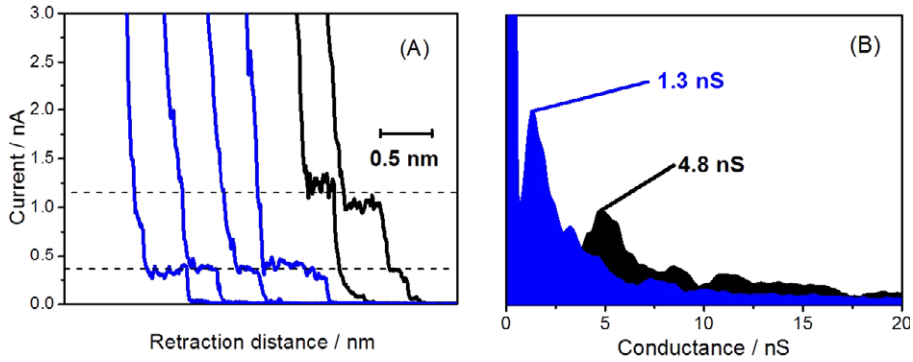

Figure 4. (A) Typical current–distance retraction curves for the STM break junction method for monoether **5** with $U_{tip} = 0.2$ V; examples showing a low conductance plateau are shown in blue and high conductance in black. (B) Histograms for both low conductance (blue trace) and high conductance (black trace) events; in this plot, the high current histogram has been weighted by a factor of five, to take into account the fact that high current events occurred only 20% as often as low current events.

Table 1. Comparison of conductance data for **5** and **6**, obtained using different techniques, and published data on comparable length alkanedithiols. (Figures S3b, S4b and S4d available at stacks.iop.org/JPhysCM/24/164211/mmedia.)

Molecule (S · · · S length in nm)	**Conduct. (nS)** $I(s)$ method	**Conduct. (nS)** Sek method ([41])	**Conduct. (nS)** BJ method
5 (1.31)	1.20 ± 0.07 (from slope of figure 1(d))	1.11 ± 0.28 (from figure S4b)	1.55 ± 0.40 (lowest current peak, figure 3(b))
$HS(CH_2)_9SH$ (1.33)	0.49 ± 0.03 ([28])		
6 (1.16)	2.95 ± 0.10	2.22 ± 0.53 (from figure S4d)	4.42 ± 1.16 (from lowest current peak; figure S3b)
$HS(CH_2)_8SH$ (1.21)	1.01 ± 0.05 ([18])		

retraction, whereupon dithiol(s) can bridge the gap that results, producing peaks in the conductance histogram plot. In the original paper [8], the experiment was conducted in the presence of a solution of the molecule under test. However, in our implementation, we use a low-coverage monolayer-coated substrate as for the $I(s)$ method. We [49], and others [42], have observed that this technique also promotes the formation of junctions in which the thiol molecules occupy high-coordination sites, which produces larger junction conductances. However, a peak at lower conductance, approximately corresponding to the value measured using the $I(s)$ and $I(t)$ techniques, can also be measured in these experiments.

In the case of molecules **5** and **6**, we observed two sets of peaks in the current histograms, one at approximately the same value as seen for the $I(s)$ method and the other at approx. four times this value (table 1). Typical examples for monoether **5** are shown in figure 4 and for diether **6** in figure S2 (available at stacks.iop.org/JPhysCM/24/164211/mmedia). We assign the high conductance peak to junctions in which one of the thiol contact atoms is coordinated at a step edge or similar high-coordination site (rather than bonded to a single gold atom) as the junction cleaves, by analogy with our earlier work on alkanedithiols [18]. The factor by which the high conductance value is bigger than the low conductance value is similar to the case of the alkanedithiols. However, interestingly, for the latter we were also able to discern a still-higher conductance, assigned as due to junctions in which both thiols are at high-coordination sites [18], as also seen by other workers [8, 17, 43], but such a peak was not observed in the histograms for either **5** or **6**. For monoether **5**, the low conductance value measured by this technique is almost the same as that determined by the $I(s)$ methods, although for diether **6** it is somewhat larger. The reason for the latter discrepancy is not clear; it is possible that some interaction between the ether oxygens and the Au contacts may occur during junction formation involving **6**, and this could be more pronounced in the 'push to contact' method.

3.3. I(s) technique on self-assembled monolayers (Sek adaptation)

Finally, we used a variant of the $I(s)$ technique first used by Sek, in which a close-packed, self-assembled monolayer of dithiol molecules **5** or **6** on an Au(111) substrate is first prepared by prolonged exposure of the surface to a concentrated solution. Monoethers such as $HS(CH_2)_n$–O–$(CH_2)_m$OH ($n = 6$; $m = 7$; $n = 7$, $m = 6$) have been shown to form close-packed, upright-standing self-assembled monolayers very similar to the corresponding alkane derivatives [36], but the structures of monolayers with compounds of the type $HS(CH_2CH_2O)_nCH_2CH_2X$ (X = –H, –SH) is less clear-cut [50]. Accordingly, we first obtained XPS spectra of both low-coverage and high-coverage monolayers of diether **6** on gold substrates.

Figure S3 (supplementary information, available at stacks.iop.org/JPhysCM/24/164211/mmedia) shows the S 2p doublet region for the high-coverage phase. It can clearly be seen that there are two (overlapping) sulfur environments of similar intensity, one with binding energy corresponding to a free thiol (163.5 eV) and one to an adsorbed thiol (162.0 eV), suggesting that diether **6** forms, at least predominantly, an upright-standing monolayer when high-coverage conditions are used. In the low-coverage monolayer spectrum, the proportion of free thiol was smaller, although it was still present. A recent publication described similar XPS experiments on self-assembled monolayers of $HS(CH_2CH_2O)_3CH_2CH_2SH$ and concluded that there was very little free thiol in this case (implying molecular 'looping' such that both thiols adsorbed), but the deposition conditions used in this work (including a 15 min deposition time) were significantly different [50].

Conductance determinations were then performed on the high-coverage monolayer phases of **5** and **6** as in the $I(s)$ method [41]. An appropriate I_0 was first selected by trial and error as the lowest value which resulted in the formation of molecular junctions. Representative examples of the data obtained in such experiments are illustrated in figure S4 in the supplementary information (available at stacks.iop.org/JPhysCM/24/164211/mmedia), and the conductances derived are shown in table 1.

The overall conclusions from the data are (i) the conductances of junctions involving both **5** and **6** are significantly greater than those of the respective alkanedithiols of comparable length, (ii) that the factor by which the conductance is larger is significantly bigger for diether **6** (with two $–CH_2–$ groups replaced by –O–) than it is for monoether **5** (with only one) and (iii) the conductance of **6** is significantly greater than that of **5**, which is as expected since **6** is shorter by one atom than **5**.

3.4. Calculations

To shed light on possible reasons for the apparent increase in conductance on replacing $–CH_2–$ groups with –O–, we now discuss the results of hybrid DFT–HF calculations using Spartan 08 carried out on monoether **5** and on $HS(CH_2)_9SH$. We do not have the computational resources to include 'slabs' of gold atoms to serve as contacts in such calculations, and so these results are simply used here for illustrative purposes; clearly, the inclusion of gold contacts would be expected to perturb the orbital energies and symmetry.

There is general consensus that conductance through these and related molecules is dominated by occupied orbitals [35, 52, 53], and so we focus on these in the arguments that follow. Figure 5 summarises the calculated energies of the orbitals from the HOMO to the HOMO-4, and illustrates the key orbitals for monoether **5** and the corresponding 1,9-nonanedithiol as a representative example. The HOMO and HOMO-1 are essentially localised on the individual thiol sulfur contact atoms, while the HOMO-2 has mainly O lone pair character for **5**, but is an σ-symmetry orbital of much lower energy for 1,9-nonanedithiol. For **5** having a single chain heteroatom, the HOMO-3 is a σ-bonding orbital of low energy,

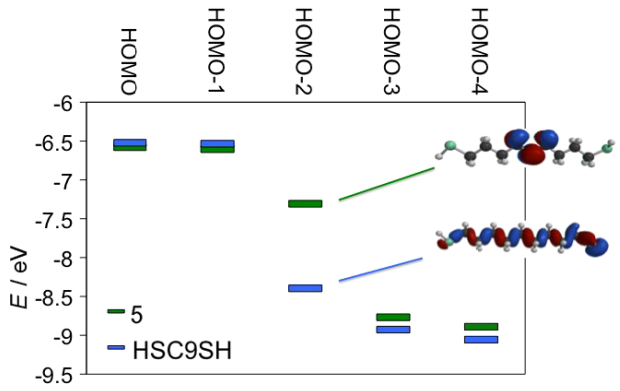

Figure 5. Energies of HOMO–HOMO-4 for monoether **5** and 1,9-nonanedithiol. HOMO-2 is a non-bonded orbital on the heteroatom for **5** and is essentially a C–C σ orbital for 1,9-nonanedithiol. HOMO-3 and HOMO-4 are σ-bonding orbitals for both molecules.

far from E_F, whereas for diether **6** it is a second heteroatom lone pair orbital (see SI figure S5, available at stacks.iop.org/JPhysCM/24/164211/mmedia). The remaining orbitals have mainly σ-bonding character and are of low energy for all of these molecules.

The heteroatom non-bonded electrons of molecules **5** and **6** are clearly closer in energy to the Au Fermi energy of the metal contacts (−5.31 eV for clean gold) than are the remaining σ orbitals of all the molecules, and we suggest that the observed higher conductances of **5** and **6** are related to the presence of these orbitals, acting in some respects as analogous to a 'well' in an inorganic double-tunnelling-barrier device when compared with the situation pertaining in the analogous $HS(CH_2)_9SH$ system. Phenyl rings may be more effective than ether oxygen atoms as 'wells' in this picture, since in molecules such as **3**, the higher-energy orbitals with arene π-bonding character are significantly closer in energy to E_F for clean gold than is the HOMO-2 of molecule **5** [35, 51].

3.5. Measurements at higher U_{tip}

The I–U behaviour of metal | molecule | metal junctions involving alkanedithiols can be fitted well by the Simmons model [54] because the frontier orbitals for such molecules are far from the Fermi energy of the contacts, and therefore the mechanism of conductance is tunnelling. Such Simmons fitting for Au | alkanedithiol | Au single-molecule junctions has been presented by Li *et al* [42] and Haiss *et al* [28]. If the ether oxygen lone pairs of **5** and **6** act as barrier indentations, it might be expected that the I–U behaviour of these molecules could deviate significantly from the Simmons model.

To investigate whether the Simmons model could be used to describe the current–voltage behaviour of **5** and **6**, the range of U_{tip} employed was increased to +1.2 to −1.2 V using the $I(s)$ method. Although typical $I(s)$ scans were often noisier at these more extreme U_{tip} owing to current-induced junction instability, good histograms were still obtained for $U_{tip} = \pm 0.8, \pm 1.0$ and ± 1.2 V. The resulting I–U curve for **5** is shown in figure 6.

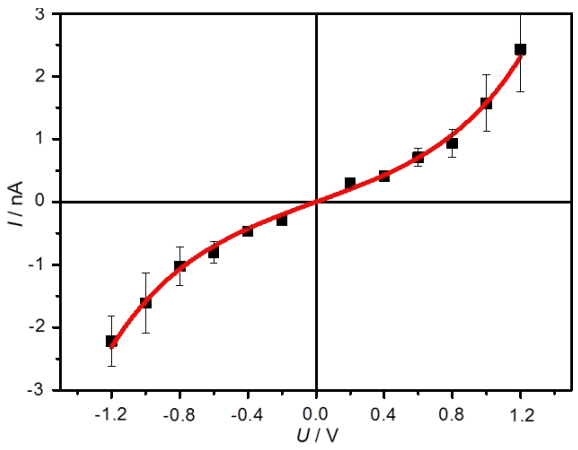

Figure 6. Current–voltage plot for **5**. The line is a Simmons fit to the data as outlined in the text.

The modified Simmons equation (equation (1)) has been widely employed to fit and understand the voltage dependence of the charge density (J) through molecular layers [54–59], and also through single molecules [28, 42]. The Simmons equation is a one-dimensional barrier-tunnelling model which may be modified to include image charge effects. In equation (1), e and m represent the charge and the mass of an electron, while d and Φ_b refer to the width and the effective height of the tunnelling barrier. α is a fitting parameter which is related to the effective mass (m_{eff}) of the tunnelling electron (or hole) where $m_e\alpha^2 = m_{\text{eff}}$:

$$J = \frac{e}{4\pi^2 h d^2} \times \left\{ \left(\Phi_B - \frac{eV}{2}\right) \exp\left[-\frac{2(2m)^{1/2}}{h}\alpha\left(\Phi_B - \frac{eV}{2}\right)^{1/2} d\right] - \left(\Phi_B + \frac{eV}{2}\right) \exp\left[-\frac{2(2m)^{1/2}}{h}\alpha\left(\Phi_B + \frac{eV}{2}\right)^{1/2} d\right] \right\}. \quad (1)$$

For the case of single molecules of **5** and **6**, J was calculated from the observed current values by assuming that the surface area occupied by a single molecule is 0.217 nm^2 (the area occupied by a single alkanethiol molecule in a $(\sqrt{3}\times\sqrt{3})$R30° self-assembled monolayer structure on Au(111)). Using equation (1) with $d = 1.5$ nm measured from the Spartan DFT calculations on **5**, a fit to the I–U data for **5** was obtained with realistic parameters, an image charge-corrected barrier height Φ_B of 0.937 eV and $\alpha = 0.50$. These may be compared with the corresponding figures for the same conductance group obtained for octanedithiol, $\Phi_B = 1.36$ eV and $\alpha = 0.53$ [28]. The barrier height for **5** is therefore significantly lower, but the conductance mechanism is similar, predominantly involving filled σ orbitals. For **6**, however, the situation is notably different. The curve was not sigmoidal and the I–U behaviour could not be modelled using the Simmons equation with physically meaningful values of the parameters Φ_B and α, and it therefore appears that the charge transport mechanism for this molecule is more complex.

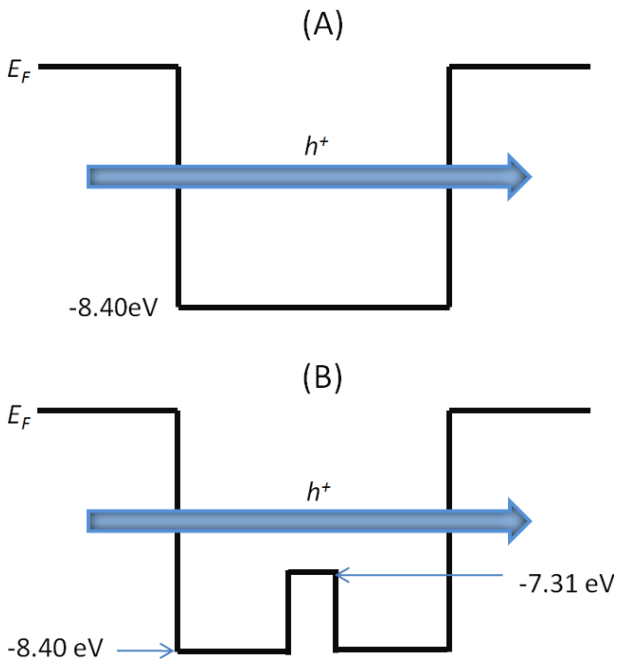

Figure 7. (A) Simple rectangular tunnelling barrier for 1,9-nonanedithiol. (B) Indented tunnelling barrier model for compound **5**. These model barriers are used in conjunction with the Gamow equation (see text).

To further illustrate the influence of a barrier indentation we take a very simple barrier-tunnelling model and the Gamow equation. A general form of the Gamow equation for tunnelling through a barrier of width a is given by equation (2), where Γ is the transparency of the barrier [60, 61]:

$$\Gamma = \exp(-\sigma) \qquad \sigma = \frac{2}{\hbar}\int_0^a \mathrm{d}x\sqrt{2m[U(x) - E]}. \quad (2)$$

In this equation $U(x) - E$ is the height of the barrier at position x, $\hbar = h/2\pi$ and m is the electron/hole mass.

The experimental single-molecule conductance data shows that the conductance of compound **5** (1.20 nS) is about 2.5 times greater than that of nonanedithiol (0.49 nS). Since these two molecules have rather comparable bond lengths this difference is accounted for by the 'barrier indentation' provided by the CH_2–**O**–CH_2 region of compound **5**, as shown in the orbital energy diagram of figure 5. We have included the barrier indentation within the framework of the Gamow model by taking the orbital energies from figure 5 for the HOMO-2 orbitals which are important frontier orbitals for compound **5** and nonanedithiol. E in the Gamow model is taken as the Fermi level of clean gold (−5.31 eV). Using the HOMO-2 energies from figure 5 a simple rectangular barrier is taken for nonanedithiol (figure 7(A)), while an indented barrier is taken for compound **5** (figure 7(B)), with the indentation spatially confined to the CH_2–**O**–CH_2 region. Using this model the conductance is predicted to increase by a factor of about 2.7 on going from the rectangular barrier of nonanedithiol to the indented barrier of compound **5**. This compares favourably with the experimentally measured factor of 2.5, given the simplicity and approximations in this model.

Note that quantitative agreement is not expected due to the simple nature of the model, which does not take account of the complex barrier profile, image charge effects, the precise position of the Fermi level and Fermi level alignment, or the effective hole mass.

In conclusion, two representative ether dithiols have been synthesised and used to fabricate metal | molecule | metal junctions, the conductances of which have been examined using a range of STM-based methods. Single-molecule junctions involving these ethers have a significantly higher conductance than otherwise analogous junctions involving alkanedithiols of the same length. We suggest that this is due to the lone pairs on the oxygen atoms acting as wells in a double-tunnelling-barrier model.

Acknowledgments

We thank the EPSRC for funding (grant EP/C00678X/1) and for funding the NCESS Service, and Dr Graham Beamson (NCESS, Daresbury) for experimental assistance and advice.

References

[1] Reed M A, Zhou C, Muller C J, Burgin T P and Tour J M 1997 *Science* **278** 252
[2] Kergueris C, Bourgoin J P, Palacin S, Esteve D, Urbina C, Magoga M and Joachim C 1999 *Phys. Rev.* B **59** 12505
[3] Weber H B, Reichert J, Ochs R, Beckmann D, Mayor M and Löhneysen H v 2003 *Physica* E **18** 231
[4] Reichert J, Ochs R, Beckmann D, Weber H B, Mayor M and von Lohneysen H 2002 *Phys. Rev. Lett.* **88** 176804
[5] Park H, Lim A K L, Alivisatos A P, Park J and McEuen P L 1999 *Appl. Phys. Lett.* **75** 301
[6] Gruter L, Gonzalez M T, Huber R, Calame M and Schonenberger C 2005 *Small* **1** 1067
[7] Yazdani A, Eigler D M and Lang N D 1996 *Science* **272** 1921
[8] Xu B Q and Tao N J 2003 *Science* **301** 1221
[9] Dorogi M, Gomez J, Osifchin R, Andres R P and Reifenberger R 1995 *Phys. Rev.* B **52** 9071
[10] Haiss W, van Zalinge H, Higgins S J, Bethell D, Höbenreich H, Schiffrin D J and Nichols R J 2003 *J. Am. Chem. Soc.* **125** 15294
[11] Haiss W, Nichols R J, van Zalinge H, Higgins S J, Bethell D and Schiffrin D J 2004 *Phys. Chem. Chem. Phys.* **6** 4330
[12] Cui X D, Primak A, Tomfohr J, Sankey O F, Moore A L, Moore T A, Gust D, Harris G and Lindsay S M 2001 *Science* **294** 571
[13] Leatherman G, Durantini E N, Gust D, Moore T A, Moore A L, Stone S, Zhou Z, Rez P, Liu Y Z and Lindsay S M 1999 *J. Phys. Chem.* B **103** 4006
[14] McCreery R L, Viswanathan U, Kalakodimi R P and Nowak A M 2006 *Faraday Discuss.* **131** 33
[15] Lindsay S M and Ratner M A 2007 *Adv. Mater.* **19** 23
[16] Hu Y B, Zhu Y, Gao H J and Guo H 2005 *Phys. Rev. Lett.* **95** 156803
[17] Li C, Pobelov I, Wandlowski T, Bagrets A, Arnold A and Evers F 2008 *J. Am. Chem. Soc.* **130** 318
[18] Haiss W, Martin S, Leary E, van Zalinge H, Higgins S J, Bouffier L and Nichols R J 2009 *J. Phys. Chem.* C **113** 5823
[19] Jones D R and Troisi A 2007 *J. Phys. Chem.* C **111** 14567
[20] Haiss W, van Zalinge H, Bethell D, Ulstrup J, Schiffrin D J and Nichols R J 2006 *Faraday Discuss.* **131** 253
[21] Cao H, Jiang J, Ma J and Luo Y 2008 *J. Am. Chem. Soc.* **130** 6674
[22] Leary E *et al* 2009 *Phys. Rev. Lett.* **102** 086801
[23] Martin S, Haiss W, Higgins S J and Nichols R J 2010 *Nano Lett.* **10** 2019
[24] Doneux T, Bouffier L, Mello L V, Rigden D J, Kejnovska I, Fernig D G, Higgins S J and Nichols R J 2009 *J. Phys. Chem.* C **113** 6792
[25] Haiss W, Zalinge H V, Höbenreich H, Bethell D, Schiffrin D J, Higgins S J and Nichols R J 2004 *Langmuir* **20** 7694
[26] Haiss W *et al* 2007 *J. Phys. Chem.* B **111** 6703
[27] Leary E, Higgins S J, van Zalinge H, Haiss W, Nichols R J, Nygaard S, Jeppesen J O and Ulstrup J 2008 *J. Am. Chem. Soc.* **130** 12204
[28] Haiss W, Martin S, Scullion L E, Bouffier L, Higgins S J and Nichols R J 2009 *Phys. Chem. Chem. Phys.* **11** 10831
[29] Chang L L, Esaki L and Tsu R 1974 *Appl. Phys. Lett.* **24** 593
[30] Ismail K, Antoniadis D A and Smith H I 1989 *Appl. Phys. Lett.* **55** 589
[31] Tsuchiya M and Sakaki H 1986 *Appl. Phys. Lett.* **49** 88
[32] Brown E R, Sollner T, Goodhue W D and Parker C D 1987 *Appl. Phys. Lett.* **50** 83
[33] Tewordt M, Martinmoreno L, Nicholls J T, Pepper M, Kelly M J, Law V J, Ritchie D A, Frost J E F and Jones G A C 1992 *Phys. Rev.* B **45** 14407
[34] Liu W C, Lour W S and Wang Y H 1992 *IEEE Trans. Electron Devices* **39** 2214
[35] Leary E, Higgins S J, van Zalinge H, Haiss W and Nichols R J 2007 *Chem. Commun.* 3939
[36] Cheng J, Saghi-Szabo G, Tossell J A and Miller C J 1996 *J. Am. Chem. Soc.* **118** 680
[37] Napper A M, Liu H Y and Waldeck D H 2001 *J. Phys. Chem.* B **105** 7699
[38] Alexander K and Schniepp L E 1948 *J. Am. Chem. Soc.* **70** 1839
[39] Nichols R J, Haiss W, Higgins S J, Leary E, Martin S and Bethell D 2010 *Phys. Chem. Chem. Phys.* **12** 2801
[40] Martín S, Giustiniano F, Haiss W, Higgins S J, Whitby R J and Nichols R J 2009 *J. Phys. Chem.* C **113** 18884
[41] Sek S, Swiatek K and Misicka A 2005 *J. Phys. Chem.* B **109** 23121
[42] Li X L, He J, Hihath J, Xu B Q, Lindsay S M and Tao N J 2006 *J. Am. Chem. Soc.* **128** 2135
[43] Fujihara M, Suzuki M, Fujii S and Nishikawa A 2006 *Phys. Chem. Chem. Phys.* **8** 3876
[44] Nishikawa A, Tobita J, Kato Y, Fujii S, Suzuki M and Fujihara M 2007 *Nanotechnology* **18** 424005
[45] Quek S Y, Kamenetska M, Steigerwald M L, Choi H J, Louie S G, Hybertsen M S, Neaton J B and Venkataraman L 2009 *Nature Nanotechnol.* **4** 230
[46] Kamenetska M, Quek S Y, Whalley A C, Steigerwald M L, Choi H J, Louie S G, Nuckolls C, Hybertsen M S, Neaton J B and Venkataraman L 2010 *J. Am. Chem. Soc.* **132** 6817
[47] Wang C S, Batsanov A S, Bryce M R, Mártin S, Nichols R J, Higgins S J, García-Suárez V M and Lambert C J 2009 *J. Am. Chem. Soc.* **131** 15647
[48] Martín S, Haiss W, Higgins S J, Cea P, López M C and Nichols R J 2008 *J. Phys. Chem.* C **112** 3941
[49] Haiss W, Nichols R J, Higgins S J, Bethell D, Höbenreich H and Schiffrin D J 2004 *Faraday Discuss. Chem. Soc.* **125** 179
[50] Snow A W, Foos E E, Coble M M, Jernigan G G and Ancona M G 2009 *Analyst* **134** 1790
[51] Brooke C, Higgins S J and Nichols R J 2010 unpublished work

[52] Reddy P, Jang S Y, Segalman R A and Majumdar A 2007 *Science* **315** 1568
[53] Venkataraman L, Park Y S, Whalley A C, Nuckolls C, Hybertsen M S and Steigerwald M L 2007 *Nano Lett.* **7** 502
[54] Simmons J G 1963 *J. Appl. Phys.* **34** 1793
[55] Wang W, Lee T R and Reed M A 2005 *Rep. Prog. Phys.* **68** 523
[56] Holmlin R E, Ismagilov R F, Haag R, Mujica V, Ratner M A, Rampi M A and Whitesides G M 2001 *Angew. Chem. Int. Edn* **40** 2316
[57] Selzer Y, Salomon A and Cahen D 2002 *J. Phys. Chem.* B **106** 10432
[58] Davis J J, Peters B and Xi W 2008 *J. Phys.: Condens. Matter* **20** 374123
[59] Wang G, Kim T W, Jang Y H and Lee T 2008 *J. Phys. Chem.* C **112** 13010
[60] Gamow G 1929 *Z. Phys.* **53** 601
[61] Kuznetsov A M and Ulstrup J 1999 *Electron Transfer in Chemistry and Biology: An Introduction to the Theory* (Chichester: Wiley)